Optical bistability and stationary patterns in photonic-crystal vertical-cavity surface-emitting lasers

Maurizio Dabbicco,[a)] Tommaso Maggipinto, and Massimo Brambilla
INFM Regional Laboratory LIT[3] and Dipartimento Interateneo di Fisica "M. Merlin" dell'Università e del Politecnico di Bari, via Amendola 173, I-70126 Bari, Italy

(Received 26 July 2004; accepted 23 November 2004; published online 6 January 2005)

We report the experimental observation of optical bistability and coherent transverse pattern formation in optically injected, photonic-crystal vertical-cavity surface-emitting lasers, electrically biased below threshold. For injected frequency blueshifted with respect to the cavity resonance, the system exhibits optical bistability and the injected uniform plane-wave breaks up, giving rise to honeycomb- and rolls-like transverse patterns. By comparison with numerical simulations we associate the observed phenomena with the onset of a modulational instability, and discuss the application of this device as an optical memory based on the cavity soliton concept. © *2005 American Institute of Physics*. [DOI: 10.1063/1.1853509]

Vertical-cavity surface-emitting lasers (VCSELs) are inherently one-dimensional (1D) photonic band gap devices along the longitudinal direction. The single axial optical mode allowed by the λ cavity can in fact be regarded as a *deep level* in the 1D photonic band gap determined by the distributed cavity mirrors (DBRs). However, in the transverse plane, broad area VCSELs naturally exhibit translational symmetry and a spatiotemporal dynamics determined by a large number of transverse modes. Even though the competition among transverse modes is usually detrimental for the coherence of the laser emission, under proper conditions, it gives rise to stationary, highly symmetrical optical patterns.[1] The direct extension of the photonic-crystal concept to the cross section of the device has led to various approaches attempting to control the transverse mode dynamics in VCSELs:[2] from drilling deep holes in the top distributed Bragg reflector (DBR)[3] to patterning the reflectivity of one of the mirrors by selective metal evaporation.[4] In either case an intentional point-defect is created that breaks the periodic modulation of the refractive index in the cross section of the VCSEL thus confining light in a single transverse mode.

Instead of being interested in the modal pattern above the laser threshold, we focused our attention to the modal behavior of photonic-crystal VCSELs (PCSELs) biased below the laser threshold, but above the transparency carrier density. In this excitation regime, the inverted population provides a steady energy storage which equally feeds all transverse cavity modes in the narrow spectral range of the cavity linewidth, and the PCSEL performs like a uniformly excited nonlinear Fabry–Perot cavity. It is well known that a semiconductor Fabry–Perot cavity develops optical bistability,[5] and, under quite general circumstances,[6] the interplay of the nonlinearity with diffraction can also give rise to a modulational instability. When a system crosses the modulational instability threshold, various interesting scenarios of modal pattern competition emerge, including: winner-takes-all dynamics, cooperation, time alternation, localization, or even space–time chaos.[7]

In this letter we report the experimental observation of optical bistability and modulational instabilty in PCSELs. The experimental results are in very good agreement with preliminary theoretical calculations, and the results of numerical simulations open perspectives for innovative applications of these devices in the field of optical information processing.

The metallorganic-vapor-phase-epitaxy-grown, top-emitting PCSELs under investigation were designed for emission near 960 nm. The AlGaAs λ cavity with three InGaAs quantum wells is followed on the *p*-side by a $\lambda/2$ layer containing a 25-nm-thick AlAs oxidation layer at the minimum of the optical field. The top DBR consists of 19 periods of *p*-doped GaAs–AlGaAs $\lambda/4$ layers, whereas the bottom DBR consists of 30 periods of *n*-doped GaAs–AlGaAs $\lambda/4$ layers. Electrical confinement and improved heat dissipation are achieved with a 10 μm lateral wet-oxidation of the AlAs layer. The periodic spatial modulation of the cavity reflectivity is achieved by means of a GaAs cap layer grown on top of the mesa and by evaporation of the *p*-electrical contact in the form of a metal grid. The grid defines 8×8 elements of $4\times 4\ \mu\text{m}^2$, separated by 1 μm metal stripes. The chosen thickness of $\sim$180 nm of the cap layer provides about 2% reflectivity modulation.[8]

The experimental setup is the same as reported in detail in Ref. 9. Briefly, the output of cw Ti:sapphire laser of wavelength $\lambda_0=2\pi c/\omega_0$ was tuned near the PCSEL resonance ($\lambda_c=2\pi c/\omega_c$), and loosely focused with a beam waist of $\sim$60 μm. The packaged device was mounted onto a Peltier cooling stage and biased below the laser threshold by a low-noise dc current. The biasing of the PCSEL in the transparency region provided the required nonlinearity while reducing the optical power necessary to achieve the optical bistability or modulational instability threshold. The light reflected from the cavity was characterized in terms of integrated intensity and near-field patterns. The measured cavity resonance was $\lambda_c=964.42\pm 0.01$ nm with half-width at half-maximum $\kappa=167\pm 5$ GHz. All measurements were taken under steady state excitation.

In Fig. 1 we show the observed near-field for different values of the cavity detuning $\theta=(\omega_c-\omega_0)/\kappa$, obtained at fixed bias current and optical excitation of $I_b=16$ mA

[a)]Electronic mail: dabbicco@fisica.uniba.it

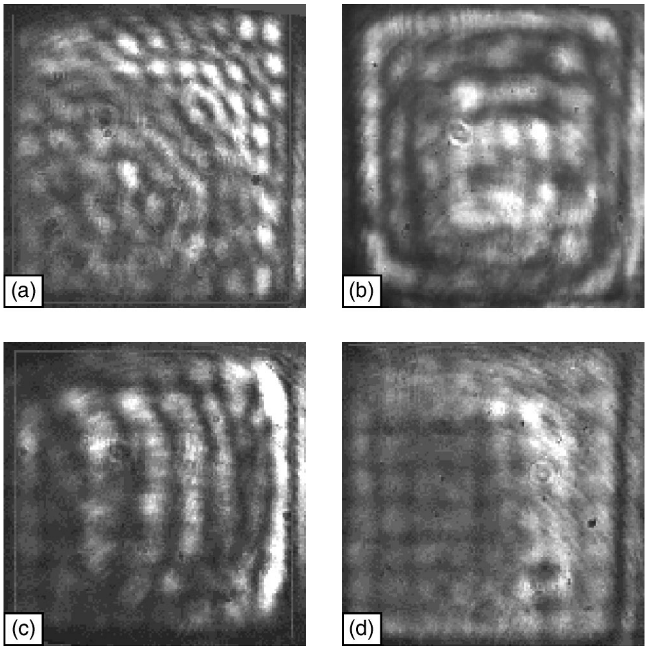

FIG. 1. Transverse optical patterns observed in the near-field imaging of the PCSEL surface for different injected wavelength, corresponding to a cavity detuning θ: −1.5 (a), −1.2 (b), −0.8 (c), −0.6 (d).

$(I_b/I_{\mathrm{th}}=0.9)$ and $P_0=200\ \mu\mathrm{W}$, respectively. Different patterns show up for $-2<\theta<-0.8$. At large negative detuning [Fig. 1(a)] a complex pattern appears that looks like the honeycomb structures often predicted in simulations of active devices.[10] The square-like pattern observed at $\theta=-1.2$ [Fig. 1(b)] is clearly affected by the grid symmetry and it is never realized in numerical simulations which consider infinite sample cross-section or periodic boundaries. By tuning the injected field closer to the cavity resonance, the frequently observed roll-like pattern emerges at $\theta=-0.8$ [Fig. 1(c)], whereas a further reduction of the detuning causes the systems to jump on to the homogeneous state [Fig. 1(d)]. Although the patterns appear to be distorted by the boundaries and by the identified gradients in the cavity frequency and current distribution across the sample area,[9] they evolve from the simpler toward the more complex structure for increasingly negative detuning, according to the quite general behavior in nonlinear resonators.[11]

In itself, this is a direct experimental observation of a modulational instability in a semiconductor microresonator with spatially modulated reflectivity. Previous experiments considering the effects of a spatially modulated feedback have been either performed in slow-response materials, like liquid[12] or photorefractive crystals,[13] or materials of problematical integration with semiconductor technology, like gas vapors.[14] However, the relevance of the present results is not limited to the field of optical instability in transverse nonlinear optics, where they demonstrate that the modulation of the cavity reflectivity imposed by the metal grid preserves the global coherence of the system. These results also put forward the PCSEL concept in the vastly explored region of optical information processing, where optical bistability is quite a general requirement for any device suitable for applications. In fact, in the same frequency range where patterns appeared, the PCSEL also showed optical bistability, as reported in Fig. 2(a).

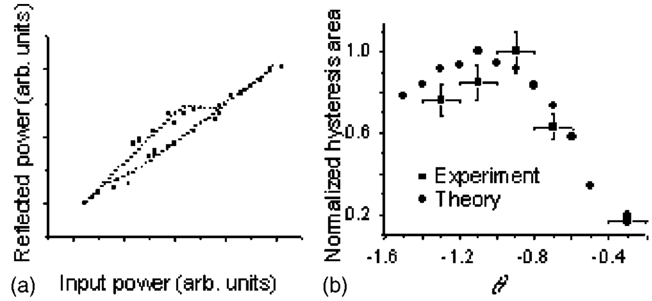

FIG. 2. (a) Experimental optical bistability measured at $\theta=-1.3$. (b) Measured and calculated area of the bistability loop as a function of the cavity detuning.

Before commenting on the relevance of these results, we compare the experiments with the theoretical predictions based on the model of Ref. 10 properly adapted to account for the modulation of the cavity transmission in the PCSEL. For the same set of the model parameters used in Ref. 10, we calculated the area of the hysteresis in the input–output intensity of the homogeneous (plane-wave) solution, as a function of the cavity detuning. The comparison with the corresponding experimental values is shown in Fig. 2(b), and it is quite satisfactory considering that no fitting parameters have been used. Moreover, numerical simulations considering a slightly larger square PCSEL of 10×10 pixels, with the same aperture:stripe ratio (4:1) of the metal grid and a 5% amplitude modulation, returned stationary optical patterns remarkably similar to the experimental ones, as shown in Fig. 3.

The concurrence of modulational instability and optical bistability is often seen as the sufficient condition for the existence of cavity solitons (CSs).[15] CSs can be thought of as self-confined structures generated by shining a narrow laser pulse into the coherently driven nonlinear cavity, so that localized high intensity peaks appear in a homogeneous background of radiation of much lower intensity. In the presence

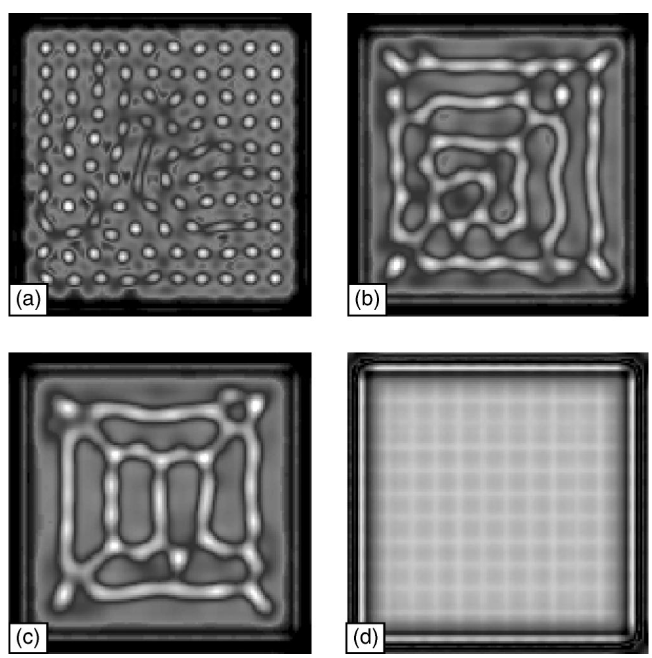

FIG. 3. Transverse optical patterns generated by numerical simulations, as described in the text, for increasing values of the cavity detuning from (a) to (d).

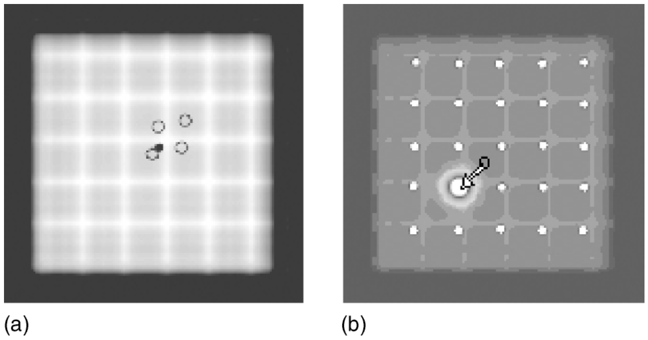

FIG. 4. Numerical simulation of the CS dynamics: device size and the model parameters are the same as in Fig. 3, except for the aperture:stripe ratio that has been doubled. (a) CSs individually addressed at different nearby locations (open circles) converge toward the nearest attractor site (black dot). (b) Actual size of one CS in its final stationary position after shifting from the switch-on location (white open circle). White dots show the regular pattern of all the complete attractors grid.

of optical bistability, CSs have been recently demonstrated to stay in the *on* state, without undergoing diffraction or dimming, until targeted by a suitable switch *off* pulse.[16] Moreover CSs appear as mobile light pixels that can be displaced and led to controlled interaction by means of phase or amplitude gradients[17] applied to the driving beam, using, e.g., reconfigurable diffractive optics. On the other hand, native frequency gradients of the cavity resonance, or phase inhomogeneities due to layer fluctuations, like those typically found in epitaxially grown VCSELs, can affect the soliton spatial stability and the ability to control their motion.[18] It is in this respect that the PCSELs can represent an attractive alternative to broad-area VCSELs, since the phase modulation can be incorporated in the device without the need for additional processing steps or external optical elements, in such a way to define $N \times M$ individually addressable permanent memory locations. To validate this concept we ran numerical simulations aimed at exploring the model parameter space in search for CSs. We found a relatively narrow range of the input field intensity where CSs exist for the same detuning of Fig. 3(b), and then intentionally addressed the switch *on* pulse to a nonsymmetrical location on the grid. As we show in Fig. 4(a), the CS shifts toward a fixed attractor point regardless of its initial position within the attractor basin, and then stays on that "memory" location. The actual position of the attractor is defined by the interaction of the CS profile with the complex nonlinear phase and intensity distribution across the PCSEL, and does not coincide with the grid nodes. However, as expected, the attractor sites are evenly distributed and form an *attractors grid* that appears diagonally rigidly translated a few microns from the *metal grid* [Fig. 4(b)]. This predicted combination of CS mobility and grid-induced pinning, for easily accessible experimental conditions (remarkably similar to that of Ref. 10), allows for conceiving simpler schemes for plastic, dynamically reconfigurable pixel arrays.

In conclusion, we have reported experimental evidence of optical bistability and stationary patterns in photonic crystal VCSELs electrically biased below the laser threshold. Such patterns emerge from the self-organization in the transverse profile of the optical intracavity field, which appears to be influenced but not dominated by the symmetry breaking of the contact grid. Numerical simulations confirmed the experimental results and allow us to foresee that localized structures should be observable in these devices.

This work was supported by Ministero dell'Università e della Ricerca (MIUR) under project FIRB-RBAUO1E855. The Authors wish to thank Dr. Sven Eitel of Avalon Photonics LTD for providing the samples and Leonardo Amato for his contribution to the early stage of this work.

[1] S. P. Hegarty, G. Huyet, J. G. McInerney, and K. D. Choquette, Phys. Rev. Lett. **82**, 1434 (1999); T. Ackemann, S. Barland, J. R. Tredicce, M. Cara, S. Balle, R. J. Jäger, M. Grabherr, M. Miller, and K. J. Ebeling, Opt. Lett. **25**, 814 (2000); J. Scheuer, M. Orenstein, and D. Arbel, J. Opt. Soc. Am. B **19**, 2384 (2002).
[2] P. S. Ivanov, H. J. Unold, R. Michalzik, J. Maehnss, K. J. Ebeling, and I. A. Sukhoivanov, J. Opt. Soc. Am. B **20**, 2442 (2003).
[3] D.-S. Song, Y.-J. Lee, H.-W. Choi, and Y.-H. Lee, Appl. Phys. Lett. **82**, 3182 (2003); A. J. Danner, J. J. Raftery, Jr., N. Yokouchi, and K. D. Choquette, *ibid.* **84**, 1031 (2004).
[4] A. Golshani, H. Pier, E. Kapon, and M. Moser, J. Appl. Phys. **85**, 2454 (1999); G. Guerrero, D. L. Boiko, and E. Kapon, Appl. Phys. Lett. **84**, 3777 (2004).
[5] E. Garmire, IEEE J. Sel. Top. Quantum Electron. **6**, 1094 (2000).
[6] L. A. Lugiato, M. Brambilla, and A. Gatti, in *Advances in Atomic, Molecular and Optical Physics* (Academic, New York, 1998), Vol. 40, p. 229.
[7] F. T. Arecchi, S. Boccaletti, and P. Ramazza, Phys. Rep. **318**, 1 (1999).
[8] F. Monti di Sopra, M. Brunner, H.-P. Gauggel, H. P. Zappe, M. Moser, R. Hövel, and E. Kapon, Appl. Phys. Lett. **77**, 2283 (2000).
[9] M. Dabbicco, L. Amato, T. Maggipinto, and M. Brambilla, Proc. SPIE **5453**, 249 (2004).
[10] L. Spinelli, G. Tissoni, M. Brambilla, F. Prati, and L. A. Lugiato, Phys. Rev. A **58**, 2542 (1998).
[11] J. B. Geddes, R. A. Indik, J. W. Moloney, and W. J. Firth, Phys. Rev. A **50**, 3471 (1994).
[12] S. Residori, T. Nagaya, and A. Petrossian, Europhys. Lett. **63**, 531 (2003).
[13] T. Carmon, M. Soljačić, and M. Segev, Phys. Rev. Lett. **89**, 183902 (2002).
[14] B. Schapers, T. Ackemann, and W. Lange, IEEE J. Quantum Electron. **39**, 227 (2003).
[15] T. Maggipinto, M. Brambilla, and W. J. Firth, IEEE J. Quantum Electron. **39**, 206 (2003).
[16] S. Barland, J. R. Tredicce, M. Brambilla, L. A. Lugiato, S. Balle, M. Giudici, T. Maggipinto, L. Spinelli, G. Tissoni, T. Knödl, M. Miller, and R. J. Jäger, Nature (London) **419**, 699 (2002).
[17] Computational nonlinear and quantum optics group (Universty of Strathclyde), http://cnqo.phys.strath.ac.uk/Movies/index.html; M. Brambilla, T. Maggipinto, I. M. Perrini, L. Spinelli, and G. Tissoni, Proc. SPIE **4283**, 551 (2001).
[18] X. Hachair, S. Barland, L. Furfaro, M. Giudici, S. Balle, J. R. Tredicce, M. Brambilla, T. Maggipinto, I. M. Perrini, G. Tissoni, and L. Lugiato, Phys. Rev. A **69**, 043817 (2004).